

Artificial neural network for cervical abnormalities detection on computed tomography images

Erlinda Ratnasari Putri¹, Ahmad Zarkasi¹, Prawito Prajitno², Djarwani Soeharso Soejoko²

¹Department of Physics, Faculty of Mathematics and Natural Sciences, Mulawarman University, Samarinda, Indonesia

²Department of Physics, Faculty of Mathematics and Natural Sciences, Universitas Indonesia, Depok, Indonesia

Article Info

Article history:

Received Feb 16, 2022

Revised Jul 4, 2022

Accepted Aug 2, 2022

Keywords:

Artificial neural network

Cervical cancer

Computed tomography

Gray level co-occurrence matrix

Snake model

ABSTRACT

Cervical cancer is the second deadliest after breast cancer in Indonesia. Sundry diagnostic imaging modalities had been used to decide the location and severity of cervical cancer, one among those is computed tomography (CT) Scan. This study handles a CT image dataset consisting of two categories, abnormal cervical images of cervical cancer patients and normal cervix images of patients with other diseases. It focuses on the ability of segmentation and classification programs to localize cervical cancer areas and classify images into normal and abnormal categories based on the features contained in them. We conferred a novel methodology for the contour detection round the cervical organ classified with artificial neural network (ANN) which was employed to categorize the image data. The segmentation algorithm used was a region-based snake model. The texture features of the cervical image area were arranged in the form of gray level co-occurrence matrix (GLCM). Support vector machine (SVM) had been added to determine which algorithm was better for comparison. Experimental results show that ANN model has better receiver operating characteristic (ROC) parameter values than SVM model's and existing approach's regarding 96.2% of sensitivity, 95.32% of specificity, and 95.75% of accuracy.

This is an open access article under the [CC BY-SA](https://creativecommons.org/licenses/by-sa/4.0/) license.



Corresponding Author:

Erlinda Ratnasari Putri

Department of Physics, Faculty of Mathematics and Natural Sciences, Mulawarman University

Barong Tongkok Street, Samarinda, Indonesia

Email: erlinda.putri@fmipa.unmul.ac.id

1. INTRODUCTION

Cervical cancer patients are the fourth most female cancer patients in the world. In Indonesia, it is the second deadliest after breast cancer [1]. It occurs in 24.5 out of 100,000 women annually [2]. Unfortunately, the risk of cervical cancer is not widely known. People with cervical cancer generally do not have major symptoms.

Digital imaging technology is advancing rapidly with a variety of applications, one of which is in the medical field, such as digital imaging identification. One of the predominantly used methods is the segmentation and classification method, which is widely used for various cancers, including cervical cancer. To determine the area and volume of cervical cancer, accurate analysis and interpretation are required to determine the extent of cervical cancer in the patient's body and provide appropriate treatment. Cervical cancer image segmentation studies have been performed with different types of imaging, including Pap smear [3]–[6], magnetic resonance imaging (MRI) [7]–[10], ultrasound [11], [12], and positron emission tomography/computed tomography (PET/CT) images [13], [14]. However, only a few segmentation studies use CT imaging data for cases of cervical cancer, such as [15].

Artificial intelligence (AI) technologies, including machine learning (ML) and deep learning (DL), are useful in developing a diagnosis of cervical cancer. AI-based clinical approaches to a cervical cancer diagnosis can be as accurate as humans, save radiation therapists time, and perform clinical identification faster and cheaper than standard methods. One of examples of the application of deep learning (DL) in the field of radiodiagnostic is the use of convolutional neural network (CNN) for the segmentation and classification of image data [10], [12], [15], [16]. However, the prediction results of any model which is applied in the field of Medical Physics are only as a second opinion to support the doctor's diagnoses and decisions.

In Indonesia, most patients with cervical cancer will see doctors after having terminal cancer. It is because not all regions in Indonesia have hospital facilities with complete radiodiagnostic modalities, one of which is MRI. In general, hospitals in Indonesia only have radiographs and CT scans. Sophisticated modalities exist only in downtown hospitals. It becomes a problem if doctors want to see a clearer image of the patient. Visualizeation on CT images is not as detailed as depicted on magnetic resonance (MR) images.

Therefore, innovation is needed in the segmentation and the classification of normal and abnormal parts of the cervix on CT images. This program is designed to provide additional information about areas of potential cervical malformations. It is also expected that clinicians will be able to provide information on how much cervical abnormalities are spreading during the cervical abnormality determination stage. The target to use this program is regional hospitals which do not have MRI facilities but only CT-Scan facilities. Although MRI images provide better visualization of body anatomy and the location of cervical anomalies than CT images, CT images continue to dominate the diagnostic technology of Indonesian hospitals, especially remote areas in Borneo, Celebes, and Papua. The predictions from this program are intended to be one of the preliminary information for doctors in remote hospitals to determine the patient's condition. Studies using CT image data on the classification of cervical cancer are difficult that they are rarely done. CT-scan is the gold-standard diagnostic imaging modality used by doctors and medical physicists to plan radiation therapy at treatment planning system (TPS) in many hospitals.

This program made CT images clearer and areas of cervical abnormalities more distinct. We presented a novel method for the contour detection around the cervical organ in CT images classified with artificial neural network (ANN) which is used to classify the image data. ANN classification studies have been performed with different types of images, for example in [17]–[19]. Besides, [20] also used ANN to classify breast images. The regional snake model [21]–[24] was the method we used to segment the cervical region and obtain the texture features from the CT images. ANN was chosen as a classification method using texture-based feature extraction, i.e., gray level co-occurrence matrix (GLCM). GLCM was used in [7] and [14] as texture features from MR images and PET-CT images. As a comparison, the support vector machine (SVM) algorithm was also added to this classification study to determine the success rate of ANN algorithm classification.

2. METHOD

The implementation and simulation processes were carried out using MATLAB. Two-hundred-twelve CT images consisted of 106 normal images of the cervix and 106 abnormal images of the cervix. All were on 512×512 pixels. Image data was obtained from three hospitals. They were taken only from the hospital database. They were split into three data sets: a training data set, a validation data set, and a test data set. Images were randomly chosen with a composition of 50% for the training dataset (106 images), 25% for the validation dataset (53 images), and 25% for the test dataset (53 images). All data were pre-processed, segmented, feature extracted and classified. The block diagram of the proposed method is shown in Figure 1.

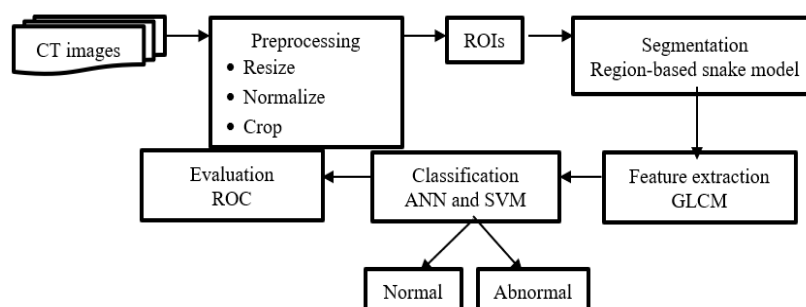


Figure 1. Flowchart of the proposed method

The preprocessing steps consisted of image resizing, normalization, and cropping. Reduce computational burden by converting digital imaging and communications in medicine (DICOM) images to tag image file format (TIFF) images. Images were then normalized, noise-reduced, and sharpened using a second-order filter. The normalized images were cropped so that the next process focuses only on the region of interest (RoI). They were then used as input to the segmentation process.

A region-based snake model was used as the segmentation method. It used energy-reducing splines to find the shape of an image object. It defined the shape of the target using energy-reducing splines to locate cervical anomalies. Many researchers believed it because of its ability to find deformations of well-segmented objects as in [17]–[19]. In (1) was the mathematical form of the local snake model [24]. I was the input image, μ_1 was the average intensity of the contoured area R1 and μ_2 was the average intensity of the outer region of R2. λ was a parameter which determines the spline smoothness.

$$E_{region}(x, y) = \lambda_1 \int_{R_1} (I - \mu_1)^2 dx + \lambda_2 \int_{R_2} (I - \mu_2)^2 dx + \lambda_3 \int_{\gamma} ds + \lambda_4 \int_{R_1} dx \quad (1)$$

In this study, no snake model control points were used at the start of the iteration. They had been replaced by a circular line which detects anomalies based on the ratio of the surrounding energy values. If there was a sufficient difference between the areal energy inside and outside the line, the algorithm stopped running and the segmentation result was displayed. However, if the edge region of the line had approximately the same energy or gray value as the region of the line, iterations continued until a sufficient energy difference was found between the two regions. The expected result was the contour line generated by the snake model algorithm representing the predicted area of cervical abnormalities and normal cervix.

Texture analysis was used as the feature extraction method. Various changes in image surface intensity were measured by the gray level match matrix (GLCM). Several previous studies, such as [7] and [14], have used texture analysis for feature extraction. The GLCM indicated whether a texture feature contained information about the spatial distribution of gray-level changes in an image. It calculated how often a pixel is associated with a particular value and a specific spatial relationship found in the image, processed the GLCM, and extracted the values from the statistical matrix to obtain the texture. Four matrices of GLCM were created with angles of 0° , 45° , 90° , and 135° . Since GLCM functions operated on the spatial domain of an image, the value of each pixel had a significant impact on the calculation of the value of GLCM parameters. Several statistics from GLCM in this study used correlation, energy, and homogeneity values to describe the texture of an image. In (2) to (4) represent the mathematical equations for each GLM function.

$$f_{correlation} = \sum_{i,j=0}^{N-1} P(i, j) \frac{(i-\mu)(j-\mu)}{\sigma^2} \quad (2)$$

$$f_{energy} = \sum_{i,j=0}^{N-1} [P(i, j)]^2 \quad (3)$$

$$f_{homogeneity} = \sum_{i,j=0}^{N-1} \frac{P(i, j)}{1+|i-j|} \quad (4)$$

While,

$$\mu = \sum_{i,j=0}^{N-1} iP(i, j) \quad (5)$$

$$\sigma^2 = \sum_{i,j=0}^{N-1} P(i, j)(i - \mu)^2 \quad (6)$$

P_{ij} was the i, j element of the normalized symmetric GLCM, i and j were the coordinates with pixel values at each position. N was the number of levels of gray available in the image. μ was the average value of GLCM, which was an estimated intensity of all the pixels connected with GLCM. σ^2 was the variance of all pixel's intensity contributing to GLCM.

Feature extraction results were used as input to ML to classify data. In this research, ANN was used for ML. It was based on the structure and function of biological neural networks. It consisted of an input layer, an intermediate layer, and an output layer. Its behavior was affected by its architecture, learning rules, and transfer functions. It had many advantages such as good learning ability, similarity to biological systems, parallelism, multi-directional execution, and reliability. ANN had succeeded in classifying categorical images based on feature identification in [17]–[19]. To strengthen this claim, the SVM algorithm was also used to determine whether the results of the classification based on the ANN algorithm were better than the results of the classification by the SVM algorithm. The principle of SVM is to find the hyperplane between two classes by choosing the hyperplane with the maximum limit.

The evaluation process in this study was carried out statistically to determine the effectiveness of problem-solving. The most common approach is receiver operating performance (ROC). In this study, ROC was used to evaluate the effectiveness of ANN and SVM. For this step, they used 212 images consisting of 106 normal images and 106 abnormal images. Of this data, 106 images were the training data set and the rest are the validation and test data sets. Images were randomly selected as part of three data sets. For the SVM algorithm, the data was only divided into two groups, namely the training data set and the testing data set. The number of images for each data set was the same, i.e. 106 images. The ROC parameters measured were sensitivity, specificity, accuracy, precision, and error. In (7) to (11) are the mathematical equations of ROC parameters measured in this study [25].

$$\text{Sensitivity} = \frac{TP}{TP+FN} \quad (7)$$

$$\text{Specificity} = \frac{TN}{TN+FP} \quad (8)$$

$$\text{Accuracy} = \frac{TP+TN}{TP+TN+FP+FN} \quad (9)$$

$$\text{Precision} = \frac{TP}{TP+FP} \quad (10)$$

$$\text{Error} = \frac{FP+FN}{TP+TN+FP+FN} \quad (11)$$

Analyses from clinicians as initial knowledge for the training process were needed at the evaluation stage. In addition, it was also required for the validation and testing data set. True positive (TP) means that software and doctors detected the image and diagnosed it as an abnormality. True negative (TN) was an image which software and doctors recognized and diagnosed as normal. False negative (FN) means that the image was detected and diagnosed normally by the software, but the doctor diagnosed the abnormality. False positive (FP) was an image which software detected and diagnosed as an abnormal image, but doctors diagnosed it as a normal image.

3. RESULTS AND DISCUSSION

This study used 212 images coming from 33 patients. These patients were from three different hospitals. One-hundred-six abnormal images were obtained from 13 cervical cancer patients and 106 normal cervical images were obtained from 20 patients with other diseases. The dose received by patients must follow the as low as reasonably achievable (ALARA) principle. Good quality images with little noise generally require a high dose. It is medical physicists who are in charge of optimizing the dose so that patients receive the minimum dose possible, but resulting images can be read by doctors properly. The dose optimization is carried out in several ways, including education of patients and radiation staff, setting the length of exploration and the number of acquisitions, the type of CT acquisition, the value of kilovoltage, and milliamps used. In addition, pitch, slice thickness, field collimator, iterative reconstructions, noise reduction filter, and active collimation also affect the dose reduction for patients [26]. It can also be helped by AI. For example, the use of AI could reduce the use of Iodine to patients to produce high-quality CT images [27].

This study did not focus on dose optimization on taking CT images of patients. The images obtained have different conditions, including brightness, sharpness, noise, slice thickness, and others. Images were obtained from one patient with a distance between image slices of 8 mm, 9 mm, 9.9 mm, and 10 mm. The first image was taken while the bladder and bowel are still visible. The first image was taken with the bladder and intestine still visible. The final image was chosen when the cervix contracted and the rectum began to emerge.

Figure 2 presents the results of each pre-processing step. Figure 2(a) is the normalized image in TIFF type. DICOM format of abnormal images was converted to TIFF format, filtered to reduce noise, sharpness, and normalized with a second-order filter. Images of the cropping process are displayed in detail. Figure 2(b) is the selected region in the image for cropping. Figure 2(c) is the result, i.e., the cropped image. It is called region of interest (RoI).

A region-based snake model was used during the segmentation process. This was described in detail in [28] and [29]. This method worked based on the inhomogeneity of image intensity using a corrected spline. To achieve contouring according to the shape of the cervix, several parameters needed to be adjusted. The number of iterations in this study ranged from 300 to 1,000. The value of time step t was 0.1. The

normalization level term set was 1, the kernel size was 5, the epsilon value did not exceed 1, and the initial constant was 2. The program displayed an external weighting constant: 1.05 and an internal weighting constant: 1. The length constant and approximate data constant α were $0.001 \times 255 \times 255$ and 20. It used a cropped image so that the segmentation process is focused only on the cervical area. Figure 3 shows the results of the segmentation process using the region-based snake model.

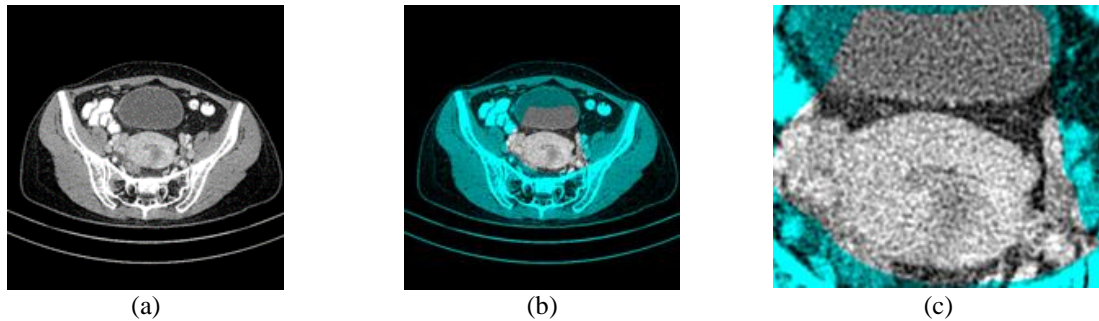


Figure 2. Pre-processing steps (a) the normalized image in TIFF type, (b) the selected region in the image for cropping, and (c) the cropped image (RoI)

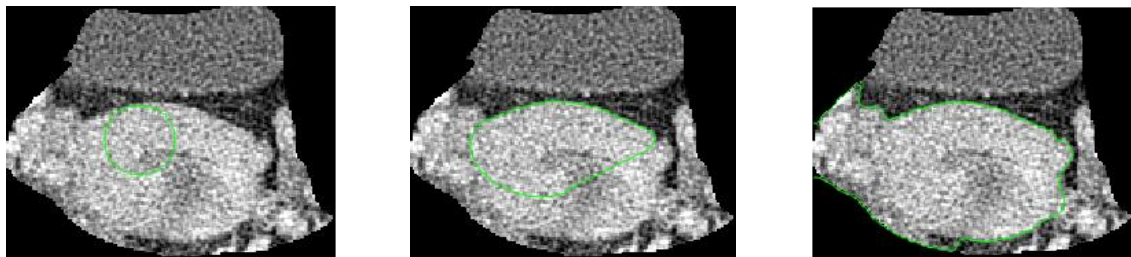


Figure 3. Results of segmentation using a region-based snake model. The green lines were the contour lines, moving iteratively and looked for the energy similarity between adjacent pixels

The later process used an image segmentation process based on this algorithm. As a result of the feature extraction process, a 212×3 feature matrix was obtained. The three features of correlation, energy, and homogeneity were obtained from all images. All features have been averaged to avoid dependence on adjacent pixels. This matrix is the input data to the ANN dan the SVM. Table 1 shows the range of values for the three features in abnormal and normal images of the cervix when training, validating and testing these images. The correlation feature values in abnormal images ranged from 0.936 to 0.967 while in normal images, the value is at 0.960-0.978. Abnormal images generally had energy feature values between 0.175 to 0.243 while the feature values for normal images were 0.190 to 0.397. The homogeneity feature values in normal images were 0.924 to 0.967. It was certainly higher than the homogeneity values in abnormal images which ranged from 0.911 to 0.935. Based on the values in Table 1, the feature values of normal images of the cervix tend to be higher than those of abnormal images of the cervix.

Table 1. Range of values of the three features in the image data

Features		Abnormal	Normal
Image data	Correlation	0.936–0.967	0.960–0.978
	Energy	0.175–0.243	0.190–0.397
	Homogeneity	0.911–0.935	0.924–0.967

In the classification process, we introduced extracted feature values as input and target values as output. Both were in matrix form. Extracted features were based on Table 1 and target values were 0 and 1. Zero means normal images and 1 means abnormal images. For the ANN algorithm, images were randomly split at a rate of 50% for the training data set, 25% for the validation data set, and 25% for the test data set. The training data set matrix consisted of 53 normal images and 53 abnormal images. The data set for

validation and testing consisted of 53 abnormal and normal images randomly. For the SVM algorithm, images were divided into two groups with the same number, namely the training data set and the testing data set. Each data set had the same number, i.e., 106 images. One-hundred-and-six images consisted of 53 normal images and 53 abnormal images which were selected randomly.

The two-layer feed-forward neural network or multilayer perceptron (MLP) was used in this step. It was able to do a non-linear mapping between the input vector and its corresponding output vector. It consisted of two layers associated with the intermediate hidden layer: the input block and the output level. This algorithm used an input layer, two hidden layers, an output layer, and an output layer. The first hidden layer consisted of 15 neurons and the second one consisted of 5 neurons. In the feedforward phase, the input was applied to the input layer and the effect was propagated layer by layer over the network until the output signal was received. It then compared the actual output of the network with the expected output and computed an error signal for each output node. Each hidden node contributed somehow to the apparent error in the output layer, so the error output was propagated from the output layer to each node in the hidden layer which contributed directly to the output layer. It was repeated layer by layer until each node in the network received an error signal which described its relative contribution to the overall error. When the error signal for each node was determined, the node used the error to update the weight values for each link until the network converged to a state it could encode all training patterns. The backpropagation algorithm used gradient descent to find the minimum of the error function in the weight space. A weight which minimized the error function was considered a solution to the training problem. In this study, we used scaled conjugate gradient backpropagation to update weight and bias values according to the scaled conjugate gradient method. Figure 4 shows the results of validating the ANN model. The best validation performance was 0.049247 at epoch 13. The cross-entropy function was used to speed up the backpropagation algorithm. The goal is to reduce loss; hence, the better the model, the smaller the loss. This function also improved overall network performance in a short time. At epoch 13, all samples in the training data set stopped updating the model's internal parameters because the error between the first and the next iteration was quite small.

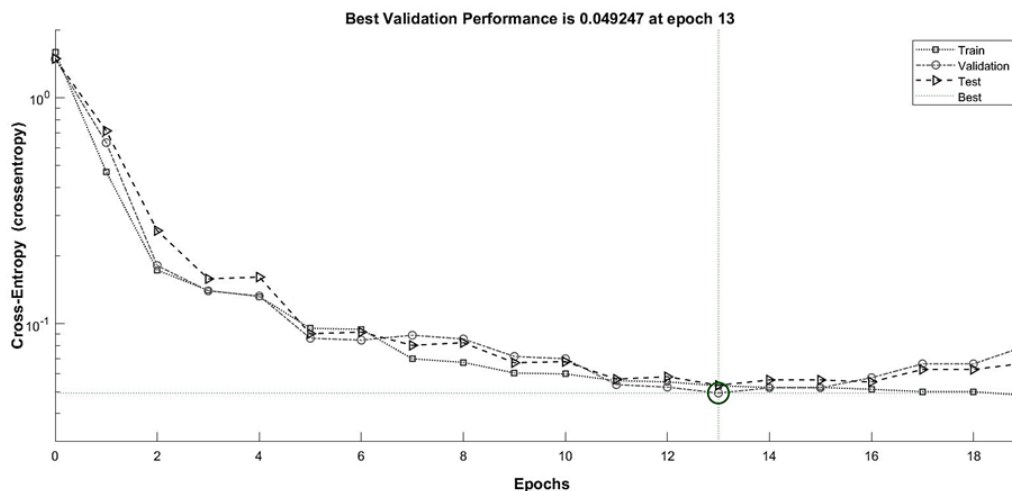


Figure 4. Cross-entropy in ANN model

The ROC analysis used to evaluate the accuracy of the ANN model in classifying images into two categories: abnormal and normal. The parameters were sensitivity, specificity, accuracy, precision, and error. Table 2 shows the performance of the ANN model. According to Table 2, the ANN model has the following performance, a sensitivity of $96.2 \pm 1.41\%$, a specificity of $95.32 \pm 1.50\%$, an accuracy of $95.75 \pm 0.81\%$, a precision of $95.28 \pm 1.66\%$, and an error of $4.25 \pm 0.81\%$. As a comparison, we classified the image data using a different algorithm, i.e., SVM. SVM worked by creating hyperplanes in a multidimensional space which separated the cases of different class labels. The type of SVM we used was binary classification. The first group was the abnormal group with 1 as an output and the other was the normal group with the value 0. Table 2 also shows the performance of the SVM model. It has the following performance, a sensitivity of $95.2 \pm 2.52\%$, a specificity of $90.5 \pm 3.53\%$, an accuracy of $92.9 \pm 2.14\%$, a precision of $90.9 \pm 3.61\%$, and an error of $7.1 \pm 2.14\%$. It indicates that the ANN model in this study is better than the SVM model because of

its good performance and stability in classifying the data. It can also be used to accurately distinguish between normal and abnormal images of the cervix.

In general, researches on cervical cancer classification used pap smear images or from datasets available on the internet. We had difficulty finding other studies using cervical CT images as material. Therefore, we compared the results of our study with those of other people who performed image classification of cervical cancer using the ANN algorithm [30]. Table 3 shows the comparison of our proposed method and existing approach in terms of performance sensitivity, specificity, and accuracy [30].

Table 2. ROC of the dataset using the ANN and the SVM algorithms

Parameter	ANN (%)	SD (%)	SVM (%)	SD (%)
Sensitivity	96.2	1.47	95.2	2.52
Specificity	95.32	1.28	90.5	3.53
Accuracy	95.75	0.74	92.9	2.14
Precision	95.28	1.44	90.9	3.61
Error	4.25	0.74	7.1	2.14

Table 3. ROC of the dataset using the ANN and the existing approach [30]

Parameter	ANN (%)	Approach [30] (%)
Sensitivity	96.2	81
Specificity	95.32	29
Accuracy	95.75	65

Although in several studies it was stated that the performance of SVM was better than ANN's, it was not the case in this study. Training of n-ary classifier with the neural network was enough to do once rather than n-ary classifier using SVM which must be trained one by one. ANN was a parametric model, while SVM was a non-parametric model. Based on the number of features and bias parameters, ANN had many hidden layers of a certain size. It helped ANN in modeling so that the classification results were almost entirely following the doctor's diagnoses.

This paper has limitations in obtaining normal and abnormal cervical CT images. For further development, more cervical CT images of various stages of cancer will be used so that the model can be tested better and the results are convincing. This image data collection can also be intended to build a database of Indonesian cervical CT images. The segmentation method will use another method. Image feature extraction will be carried out in the frequency domain using a wavelet transform. The classification method will use another algorithm with the output of several classes for cancer staging, such as CNN. Images of patients from various modalities are transferred almost instantly from the modality computer used to the electronic devices of radiologists and medical physicists via the internet. Data transmission and access are still limited based on the code of ethics so that only devices owned by interested parties can access them. The image data are collected in a cloud-based electronic personal health record which can be shared with certain providers. Institutions which require image data for research can directly access it.

4. CONCLUSION

Based at the experimental results, it can be concluded that this system can come across cervical abnormalities and classify abnormal and normal cervical images very well. The snake model gives accurate and good results for the segmentation of the cervical edge. The feature parameters used in this study were three textures, namely: correlation, energy, and homogeneity. In general, the value of three features for an abnormal image of the cervix is usually lower than the value of three features for a normal image of the cervix. The difference between the normal image and the abnormal image becomes clear through the classification process using ANN and SVM. This process also aims to classify images into abnormal and normal groups based on the features value of each image. Validating and testing processes were performed on 106 images using ROC with input in the form of a doctor's diagnosis. The ANN has better values of ROC parameters than the SVM's and the existing approach's.




ACKNOWLEDGEMENTS

This work was supported by Physical Departments of Mulawarman University and Universitas Indonesia.




REFERENCES

- [1] W. H. Organization, "Cervical Cancer," 2021. https://www.who.int/health-topics/cervical-cancer#tab=tab_1 (accessed Dec. 20, 2021).
- [2] E. S. Aoki *et al.*, "National screening programs for cervical cancer in Asian countries," *Journal of Gynecologic Oncology*, vol. 31, no. 3, 2020, doi: 10.3802/jgo.2020.31.e55.
- [3] P. Wang, J. Wang, Y. Li, L. Li, and H. Zhang, "Adaptive Pruning of Transfer Learned Deep Convolutional Neural Network for Classification of Cervical Pap Smear Images," *IEEE Access*, vol. 8, pp. 50674–50683, 2020, doi: 10.1109/ACCESS.2020.2979926.
- [4] B. Taha, J. Dias, and N. Werghi, "Classification of cervical-cancer using pap-smear images: A convolutional neural network approach," *Communications in Computer and Information Science*, vol. 723, pp. 261–272, 2017, doi: 10.1007/978-3-319-60964-5_23.
- [5] E. Hussain, L. B. Mahanta, C. R. Das, and R. K. Talukdar, "A comprehensive study on the multi-class cervical cancer diagnostic prediction on pap smear images using a fusion-based decision from ensemble deep convolutional neural network," *Tissue and Cell*, vol. 65, 2020, doi: 10.1016/j.tice.2020.101347.
- [6] B. Ashok and P. Aruna, "Comparison of Feature selection methods for diagnosis of cervical cancer using SVM classifier," *Int. Journal of Engineering Research and Applications*, vol. 6, no. 1, pp. 94–99, 2016, [Online]. Available: www.ijera.com.
- [7] M. K. Soumya, K. Sneha, and C. Arunvinodh, "Cervical cancer detection and classification using texture analysis," *Biomedical and Pharmacology Journal*, vol. 9, no. 2, pp. 663–671, 2016, doi: 10.13005/bpj/988.
- [8] G. K. Verma, J. S. Lather, and A. Kaushal, "MatConvNet-Based Fast Method for Cervical MR Images Classification," *Advances in Intelligent Systems and Computing*, vol. 799, pp. 669–679, 2019, doi: 10.1007/978-981-13-1135-2_51.
- [9] Y. C. Lin *et al.*, "Deep learning for fully automated tumor segmentation and extraction of magnetic resonance radiomics features in cervical cancer," *European Radiology*, vol. 30, no. 3, pp. 1297–1305, 2020, doi: 10.1007/s00330-019-06467-3.
- [10] Y. Kurata *et al.*, "Automatic segmentation of the uterus on MRI using a convolutional neural network," *Computers in Biology and Medicine*, vol. 114, 2019, doi: 10.1016/j.combiomed.2019.103438.
- [11] S. A. Mason *et al.*, "Towards ultrasound-guided adaptive radiotherapy for cervical cancer: Evaluation of Elekta's semiautomated uterine segmentation method on 3D ultrasound images: Evaluation," *Medical Physics*, vol. 44, no. 7, pp. 3630–3638, 2017, doi: 10.1002/mp.12325.
- [12] V. D. Soni and A. N. Soni, "Cervical cancer diagnosis using convolution neural network with conditional random field," *Proceedings of the 3rd International Conference on Inventive Research in Computing Applications, ICIRCA 2021*, pp. 1749–1754, 2021, doi: 10.1109/ICIRCA51532.2021.9544832.
- [13] W. Mu *et al.*, "A segmentation algorithm for quantitative analysis of heterogeneous tumors of the cervix with 18F-FDG PET/CT," *IEEE Transactions on Biomedical Engineering*, vol. 62, no. 10, pp. 2465–2479, 2015, doi: 10.1109/TBME.2015.2433397.
- [14] S. W. Chen *et al.*, "Textural features of cervical cancers on FDG-PET/CT associate with survival and local relapse in patients treated with definitive chemoradiotherapy," *Scientific Reports*, vol. 8, no. 1, 2018, doi: 10.1038/s41598-018-30336-6.
- [15] Z. Liu *et al.*, "Segmentation of organs-at-risk in cervical cancer CT images with a convolutional neural network," *Physica Medica*, vol. 69, pp. 184–191, 2020, doi: 10.1016/j.ejmp.2019.12.008.
- [16] R. H. Bedeir, R. O. Mahmoud, and H. H. Zayed, "Automated multi-class skin cancer classification through concatenated deep learning models," *IAES International Journal of Artificial Intelligence*, vol. 11, no. 2, pp. 764–772, 2022, doi: 10.11591/ijai.v11.i2.pp764-772.
- [17] K. Deepa and R. Dharani, "A Journal on Cervical Cancer Prediction Using Artificial Neural Networks," *Turkish Journal of Computer and Mathematics Education (TURCOMAT)*, vol. 12, no. 2, pp. 1085–1091, 2021, doi: 10.17762/turcomat.v12i2.1124.
- [18] R. D. Aldian, E. Purwanti, and M. A. Bustomi, "Applied computing based artificial neural network for classification of cervical cancer," *Applied Computing Based*, vol. 6, pp. 4–7, 2013.
- [19] M. A. Devi, S. Ravi, J. Vaishnavi, and S. Punitha, "Classification of Cervical Cancer Using Artificial Neural Networks," *Procedia Computer Science*, vol. 89, pp. 465–472, 2016, doi: 10.1016/j.procs.2016.06.105.
- [20] J. J. Patel and S. K. Hadia, "An enhancement of mammogram images for breast cancer classification using artificial neural networks," *IAES International Journal of Artificial Intelligence*, vol. 10, no. 2, pp. 332–345, 2021, doi: 10.11591/ijai.v10.i2.pp332-345.
- [21] I. El Naqa *et al.*, "Concurrent multimodality image segmentation by active contours for radiotherapy treatment planning," *Medical Physics*, vol. 34, no. 12, pp. 4738–4749, 2007, doi: 10.1118/1.2799886.
- [22] P. Yu and C. L. Poh, "Region-based snake with edge constraint for segmentation of lymph nodes on CT images," *Computers in Biology and Medicine*, vol. 60, pp. 86–91, 2015, doi: 10.1016/j.combiomed.2015.02.011.
- [23] X. Chen, B. M. Williams, S. R. Vallabhaneni, G. Czanner, R. Williams, and Y. Zheng, "Learning active contour models for medical image segmentation," *Proceedings of the IEEE Computer Society Conference on Computer Vision and Pattern Recognition*, vol. 2019–June, pp. 11624–11632, 2019, doi: 10.1109/CVPR.2019.01190.
- [24] T. F. Chan and L. A. Vese, "Active contours without edges," *IEEE Transactions on Image Processing*, vol. 10, no. 2, pp. 266–277, 2001, doi: 10.1109/83.902291.
- [25] M. Gönen, "Receiver Operating Characteristic," *SpringerReference*, vol. 31, pp. 210–231, 2011, doi: 10.1007/springerreference_63673.
- [26] A. Gervaise, P. Teixeira, N. Villani, S. Lecocq, M. Louis, and A. Blum, "CT dose optimisation and reduction in osteoarticular disease," *Diagnostic and Interventional Imaging*, vol. 94, no. 4, pp. 371–388, 2013, doi: 10.1016/j.diii.2012.05.017.
- [27] C. H. McCollough and S. Leng, "Use of artificial intelligence in computed tomography dose optimisation," *Annals of the ICRP*, vol. 49, no. 1_suppl, pp. 113–125, 2020, doi: 10.1177/0146645320940827.
- [28] C. Li, C. Y. Kao, J. C. Gore, and Z. Ding, "Minimization of region-scalable fitting energy for image segmentation," *IEEE Transactions on Image Processing*, vol. 17, no. 10, pp. 1940–1949, 2008, doi: 10.1109/TIP.2008.2002304.
- [29] L. Wang *et al.*, "Active contours driven by edge entropy fitting energy for image segmentation," *Signal Processing*, vol. 149, pp. 27–35, 2018, doi: 10.1016/j.sigpro.2018.02.025.
- [30] A. S. and S. M.V., "Classification of Cervical Cancer Cells in Pap Smear Screening Test," *ICTACT Journal on Image and Video Processing*, vol. 06, no. 04, pp. 1234–1238, 2016, doi: 10.21917/ijivp.2016.0179.




BIOGRAPHIES OF AUTHORS

Erlinda Ratnasari Putri    received her Master of Science degree from Universitas Indonesia, Indonesia in 2018. She also received her B.Sc. (Physics) from Lambung Mangkurat University, Indonesia in 2015. She is a lecturer at the Department of Physics at Mulawarman University, Indonesia. Her main research is in the medical physics area focused on interventional radiology and radiodiagnostic study. She is also skilled in digital signal processing and medical imaging. She can be contacted at email: erlinda.putri@fmipa.unmul.ac.id.






Ahmad Zarkasi    received his Bachelor of Science degree from the University of Mataram, Indonesia, in 2012 majoring in Physics. In 2017, he received his Master of Science degree from Brawijaya University, Indonesia, with the same major. Currently, he is a lecturer at the Department of Physics at Mulawarman University, Indonesia. His main research is in instrumentation physics, especially on electrical impedance tomography (EIT) and electrical impedance spectroscopy (EIS). He can be contacted at email: ahmad.zarkasi@fmipa.unmul.ac.id.



Dr. Prawito Prajitno    received his Ph.D. degree in Automatic Control and Systems Engineering from the University of Sheffield, the United Kingdom in 2002. Currently, he is a lecturer and researcher at the Department of Physics - Universitas Indonesia where he is conducting research activities in the area of computer-aided diagnosis and biomedical instrumentations. He can be contacted at email: prawito@sci.ui.ac.id.



Prof. Dr. Djarwani Soeharso Soejoko    received her bachelor's and master's degrees from the Universitas Indonesia in the field of physics of materials. She obtained her Ph.D. in the field of biophysics from the Bandung Institute of Technology (ITB). She is still active in research and teaching as well as tutoring the students in the field of medical physics. She has published many publications in her field in national and international journals. She is the founder of the Medical Physics Physics division in the Department of Physics – Universitas Indonesia. She can be contacted at email: djarwani@sci.ui.ac.id.